ADVANCED MATERIALS INTERFACES
www.advmatinterfaces.de

Antimicrobial and Antibiofouling Electrically Conducting Laser-Induced Graphene Spacers in Reverse Osmosis Membrane Modules

Lakshmi Pisharody, Chidambaram Thamaraiselvan, Emily Manderfeld, Swatantra P. Singh, Axel Rosenhahn, and Christopher J. Arnusch**

Biofouling is an ongoing challenge for water treatment membrane processes. Reducing biofilm growth on the membrane surface or on the polymeric feed spacer will reduce operation, maintenance, and module replacement costs. Laser-induced graphene (LIG) is a low cost, environmentally friendly, electrically conductive carbon material shown to have antibiofouling properties. Here it has been shown that an electrically conductive LIG-coated polypropylene (PP) feed spacer has both antimicrobial and antifouling effects under a low electrical current, and when implemented into a spiral wound membrane module reduced biofilm growth on both the membrane and the spacer components. The antibacterial property of the LIG spacer is tested using *Pseudomonas aeruginosa* and the brackish water *Rheinheimera sp.* as model organisms. Using a voltage of 12 V, *P. aeruginosa* is completely inactivated in 10 h, while a dynamic accumulation assay employing *Rheinheimera sp.* showed significant reduction ($p < 0.05$) in bacterial adhesion compared to an uncoated spacer. The spacer is incorporated into a spiral wound reverse osmosis (RO) membrane module, and reduced biofouling is observed on both the membrane and LIG spacers components using brackish water and 12 V. This study demonstrates the feasibility of electrically conductive feed spacer components in spiral wound RO membrane modules.

1. Introduction

Reverse osmosis (RO) is a membrane-based process that has been employed for various water treatment processes and desalination.[1] Pressure-driven RO processes are capable of removing almost all contaminants, however, fouling prevention is a major challenge in maintaining the RO membranes.[2,3] Various types of fouling can occur, which can be caused by colloids or particulates, or by sparingly soluble salts. However, biofouling remains a significant problem that reduces membrane performance.[4–6] Biofouling results in increased transmembrane pressure, and reduces permeate flux and salt rejection, factors that increase the cost and energy consumption of the process.[2,7–9] Biofilm formation or biofouling on a membrane surface is a multistage process that typically is slow and complex in nature. The microbial growth on the membrane resulting in

L. Pisharody, C. Thamaraiselvan,[+] S. P. Singh,[++] C. J. Arnusch
Department of Desalination and Water Treatment
Zuckerberg Institute for Water Research
The Jacob Blaustein Institutes for Desert Research
Ben-Gurion University of the Negev
Sede-Boqer Campus, Midreshet Ben Gurion 8499000, Israel
E-mail: arnusch@bgu.ac.il

The ORCID identification number(s) for the author(s) of this article can be found under https://doi.org/10.1002/admi.202201443.

[+]Present address: Interdisciplinary Centre for Energy Research, Indian Institute of Science, Bengaluru, 560012, India

[++]Present address: Environmental Science and Engineering Department, Indian Institute of Technology Bombay, 400076, India

E. Manderfeld, A. Rosenhahn
Analytical Chemistry- Biointerfaces
Ruhr University Bochum
Faculty for Chemistry and Biochemistry
44780 Bochum, Germany
E-mail: axel.rosenhahn@rub.de

DOI: 10.1002/admi.202201443

a fouled membrane occurs through a cascade of events that includes transport, deposition, and adhesion of the microbial cells, followed by the production of extracellular polymeric substances (EPS), cell growth, and proliferation. The major surface characteristics of the membrane governing the formation of biofilm on the membrane are surface wettability and roughness.[10] However, despite decades of development, current commercial membranes remain susceptible to biofilm formation and biofouling. These membranes have been highly optimized for water permeability and solute rejection, and thus commercially viable advances for the prevention of membranes fouling remains challenging. New strategies that improve other components in the module such as the membrane spacer could reduce fouling without affecting membrane performance.

Graphene has been used for a range of different applications,[11–13] due to properties such as large surface area, electrical conductivity, and mechanical stability. The material has demonstrated use for a variety of environmental applications, such as heterogeneous Fenton and electro-Fenton catalysis, biosensors, and adsorption.[14,15] Also, an array of graphene and graphene-based nanomaterials have shown antibacterial properties,[16–18] and antibiofilm effects, where biofilm growth inhibition was shown on water treatment membranes.[19–22] Graphene production includes various physical and chemical methods, such as chemical vapor deposition, epitaxial growth, oxidation–reduction of graphite, and thermal exfoliation have been developed. However, these fabrication methods can entail multiple laborious and cost-intensive steps. Also, many methods typically employ chemical agents, and their disposal results in environmental pollution.[23–25] On the contrary, laser-induced graphene (LIG) can be fabricated directly on surfaces with no additional chemical reagents or liquid waste streams.[26] The material can be easily fabricated on polymers, such as polyimide, polyether sulfone, and others that are commonly used in water filtration membranes.[27] LIG can inhibit biofilm formation and when an electric current is passed through the material, antiviral and antibacterial effects are observed.[21,28–30] Mechanisms have been suggested including physical puncturing of the cell membrane, oxidative stress that could be reactive oxygen species-dependent or independent, and direct electrical effects. However, the application of LIG on a porous membrane surface changes the membrane separation properties because the surface layers of the membrane are carbonized in the process affecting the pore size and structure. So far, coating LIG on other components in the membrane module such as feed spacers has not yet been reported.

In the present study, LIG was successfully coated on a polypropylene (PP) feed spacer and incorporated into a RO membrane spiral wound module. The antimicrobial and antibiofouling effects of the LIG-coated feed spacer were observed while applying an electric current. First, the antibacterial property of the LIG spacer was tested in the batch mode with bacteria typically observed in brackish water, and thereafter the antibiofouling effects were tested under dynamic conditions. Tests were performed under an electric potential of 12 V, and membranes were examined at constant flux with water containing a bacterial consortium isolated from the brackish water source in Israel.

2. Experimental Section

2.1. Materials

Polyimide (PI) films ≈125 mm thick were obtained from online suppliers. Luria–Bertani (LB) Broth and Bacto Agar were procured from BD (Becton, Dickinson and Company, USA). Na_2HPO_4 (VWR, USA), NH_4Cl (Merck, Germany), NaCl (Fisher Scientific, USA), and glycerol (Fisher Scientific, USA) were used as obtained. LIVE/DEAD BacLight bacterial viability kit was used from Thermo Fisher Scientific (Molecular Probes, USA).

2.2. Bacterial Strains

Pseudomonas aeruginosa (PA01) and *Rheinheimera sp*. were employed to test the antibacterial property of conductive LIG spacers in the batch mode. *Rheinheimera sp*. was cultured from a dry culture from Deutsche Sammlung von Mikroorganismen und Zellkulturen (DSMZ, Braunschweig, Germany). The bacterial concentration employed for biofouling studies was 7.5×10^6 CFU mL^{-1}. For PA01, bacterial aliquots were preserved in small stock vials with 25% glycerol at –80 °C. The content of the stock vials was thawed and streaked on LB agar plates and incubated at 37 °C for 24 h. Thereafter, a single isolated colony was harvested and grown overnight in sterile LB media at 37 °C under shaking. Also, a bacterial consortium was grown by enriching brackish groundwater collected from Mashabei Sade, Israel with 10% sterile LB. Brackish water containing 10% LB was allowed to grow for 24 h at 37 °C with shaking at 100 rpm. Thereafter the suspension was centrifuged at 6000 rpm and the bacterial pellet was again resuspended and grown in brackish water (10% LB). The cycle was repeated thrice, wherein the final bacterial pellet was resuspended in 1 M PBS buffer. The bacterial consortium was thereafter frozen and stored at –80 °C. The antibiofouling property of LIG spacers incorporated into spiral wound RO membrane modules was thereafter tested employing the bacterial consortium isolated from real brackish water.

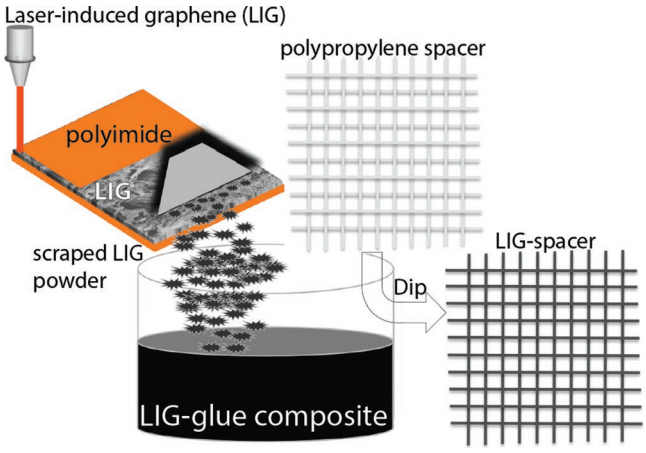

Figure 1. Schematic of the LIG powder coating on PP spacer.

2.3. Fabrication of Laser-Induced Graphene (LIG) Spacers

LIG was fabricated on PI substrates using a 10.6 µm carbon dioxide (CO_2) laser cutting system (Universal VLS 3.50 Laser cutter platform) as previously described[27,28,30,31] using the following settings: 30% power, 7% scan rate, and 1000 PPI. The LIG was scraped from the PI substrate using a microscope glass slide, and a black powder was obtained. Thereafter 5 mg of LIG powder was added to 1 mL of conductive carbon glue (Conductive Wire Glue/Paint, www.wireglue.us), stirred well with a glass rod, and sonicated for 5 min. A polypropylene (PP) feed spacer from a discarded RO module was extracted, cleaned, and immersed in 50% isopropyl alcohol and sonicated for 10 min. The cleaned spacer was then dried at room temperature for at least 2 h. The PP spacer was dipped in the LIG glue mixture and the coated spacer was dried at room temperature overnight. Approximately 10 mL of the LIG glue mixture was used to coat a 1 m^2 surface area. The schematic of the coating process is presented in **Figure 1**. For comparison, a spacer was coated with carbon glue not containing LIG. For the spiral-wound module, the membrane sheets were ≈52 cm long and 30 cm wide with a spacer thickness of 0.8 mm. Morphological analysis and the electrical resistance of the modified feed spacer were thereafter measured. The electrical resistance of the conductive spacers was measured by a two-probe multimeter (Uni-T ut33) at room temperature with the aid of copper foil to have better contact as shown in our previous work.[32] The electrical conductivity ($1/\rho$) of the LIG spacer was calculated using the following equation

$$\text{Resistivity}(\rho) = \frac{RA}{l} \tag{1}$$

Where R-resistance (Ohm), A-cross sectional area ($A = l \times w$) (m^2), l-distance (m), w-thickness (m). The thickness of the coated layer is ≈50 µm.

The morphology of the CG and LIG spacer was observed by using a scanning electron microscope (SEM) (FEI JEOL IT 200). Prior to SEM imaging, the samples were sputter coated with gold/palladium.

2.4. Fabrication of a Spiral Wound Module Containing Modified Feed Spacers

The LIG spacers (60 cm × 30 cm), were incorporated into spiral wound 1812 RO membrane modules, fabricated by Aqua

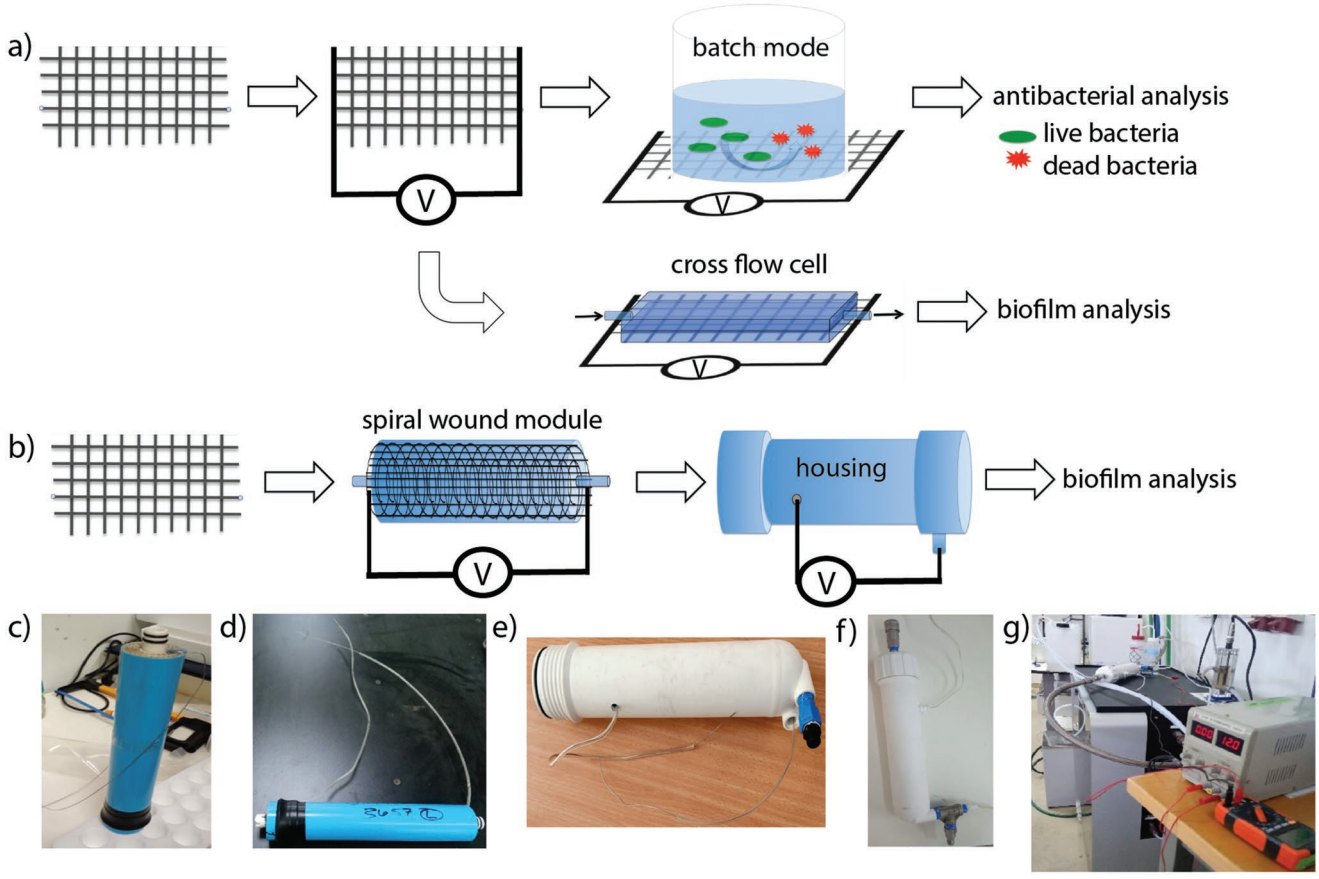

Figure 2. Schematic assembly of antimicrobial and biofilm growth assays. a) LIG spacer is connected to an electric potential and tested in batch mode for antimicrobial activity or in a cross-flow mode in a biofilm growth assay. b) LIG spacer is assembled in a spiral wound membrane module, electrical wires attached and inserted into the modified housing. c) Image of spiral wound module with wires attached. d) Wires covered with silicon tubing. e) Module inserted in customized housing. f) Fittings attached and housing sealed. g) Module assembled in a crossflow membrane testing system and wires attached to a power source (12 V).

Membranes, Inc. (Albuquerque, USA). A wire was connected at the permeate and the feed end of the module to allow the passage of current through the spiral wound module (**Figure 2**). The wires were attached to the spacer with carbon glue and strengthened with epoxy resin. To prevent the direct contact of the wire with water the steel wire was housed inside silicon tubing. Biofouling experiments were conducted with electricity (12 V) using an NF/RO crossflow system (Convergence, Netherlands).

2.5. Feed Spacer Electrical Heating Measurements

Electrical Joule heating of the LIG spacer and a spacer coated only with carbon glue were measured. Each end of the spacer (7 cm x 1 cm) was connected to a power supply (Manson NSP-3630), and a potential of 10 and 12 V was applied. The temperature increase at the surface over 6 min was measured in the air using a thermometer (Voltcraft 302 K/J).

2.6. Batch Mode Bacterial Inhibition Assay

Electrical leads were attached on both ends of the spacer (7 cm x 1 cm) and the middle of the spacer was immersed in a solution of *Pseudomonas aeruginosa* (10^6 CFU mL^{-1}) in 50 mL PBS in a sterile glass beaker without immersing the electrical contact points (see Figure S1, Supplementary Information). A voltage of 12 V (max. current ≈700 mA) was applied for 12 h. Samples were collected every 2 h and bacteria were quantified by standard plate count methods.[30]

2.7. Dynamic Accumulation Assays

Rheinheimera sp. was cultured from a dry culture from Deutsche Sammlung von Mikroorganismen und Zellkulturen (DSMZ, Braunschweig, Germany) was streaked onto an agar plate, consisting of sterile marine bouillon medium with 2% Bacto Agar (Difco, Augsburg, Germany). After 6–14 days, an individual colony was inoculated in a 7.5 mL sterile medium and allowed to grow overnight at 18 °C on an orbital shaker. The overnight culture was filtered and diluted at 1:100 in the medium. The culture was maintained at room temperature until an OD_{600} of 0.1 was attained. After centrifugation for 5 min at 3000 rpm, the pellet was resuspended in minimal media (per 1000 mL: 6 g Na_2HPO_4, 3 g KH_2PO_4, 1 g NH_4Cl, 0.5 g NaCl, 1% glycerol). Bacteria concentration was adjusted to ≈10^6 CFU mL^{-1}. The LIG feed spacer was glued to a glass slide to ensure that it was kept underwater during the measurement while keeping the front and back edges used for connection to the power source outside of the water. The samples were placed into individual compartments, and 12 V was applied (I = 0.002 A). 10 mL of the bacteria suspension was added to the compartments, and bacteria were allowed to settle for 1 h under dynamic conditions (70 rpm on an orbital shaker). Thereafter the samples were removed and placed into a glutaraldehyde bath (2.5% in Milli-Q water) for 10 min. The samples were washed two times for 10 min in Milli-Q water and subsequently stained with a LIVE/DEAD BacLight bacterial viability kit for 30 min and washed in Milli-Q again. Surfaces were allowed to dry overnight in the dark and imaged using fluorescence microscopy (Nikon CFI Plan Fluor DLL 10× NA 0.3 by Nikon, Tokyo, Japan, 10x objective with Texas red filter set) using at least 10 fields of view per sample with a Z-Stack at each point to detect all bacteria. Three individual experiments were performed. Statistical significance was tested between the LIG feed spacer without electricity and the LIG feed spacer with applied currents using the Mann-Whitney-Test ($\alpha = 0.05$). Error bars represent the standard error.

2.8. Cross-Flow Mode Plate and Frame Module Biofouling Assay

To test antibiofouling properties of a LIG-coated spacer, a previously reported membrane biofouling system was used.[31,33] Briefly, two flow-through membrane channels were operated in the continuous mode with internal recirculation through a bioreactor. The recirculation reactor (40 mL capacity) was kept at a retention time of ≈20 min, below the doubling time of the bacteria. Prior to the start of the experiments, the spacers (8 cm × 3 cm) were assembled in each of the cleaned flow cells and washed with deionized water. Next, a fresh culture of 10^4 CFU mL^{-1} *P. aeruginosa* (PA01) in distilled water was recirculated for 1 h through the membrane cell. Then the feed (bacteria contained water) and nutrients (20 ppm LB broth) mixtures were supplied by a peristaltic pump at the flow rate of 0.16 ms^{-1} to the cell and operated continuously for 72 h. From the beginning, 10 V was applied through the resistive mode (Joule heating) electrical circuit to one channel. The control channel was studied without electricity. At the end of the experiment, the spacers from both channels were carefully removed from the cells, washed with saline (0.9%), and analyzed by confocal laser scanning microscopy (CLSM) and SEM.

2.9. Spiral Wound Module Biofouling Assay

Feedwater was prepared using brackish water obtained from Mashabei Sade, Israel, containing 10% LB and 10^6 CFU mL^{-1} of the bacterial consortium. The content of the stock vials containing the bacterial consortium isolated from real brackish water was thawed and regrown in LB overnight. Thereafter, 10^6 CFU mL^{-1} bacterial suspension was added to the brackish feedwater. The feedwater containing bacteria was passed through the module in recirculation mode at a constant flux (4 LMH) and cross-flow velocity (0.1 m s^{-1}) for 4 h at R.T. Thereafter, sterile brackish water containing 10% LB was recirculated for 48 h. Pressure drop across the feed channel and permeate water flux were measured continuously. The temperature and pH of the feedwater were 25 °C and 7.5, respectively. Control tests included an identical module that was fabricated containing the uncoated spacer and a module with LIG spacer without electricity.

2.10. Membrane Autopsy and Biofilm Characterization

At the end of each run, the module was autopsied (**Figure 3**) and sections (1 cm × 1 cm) of membrane and feed spacers

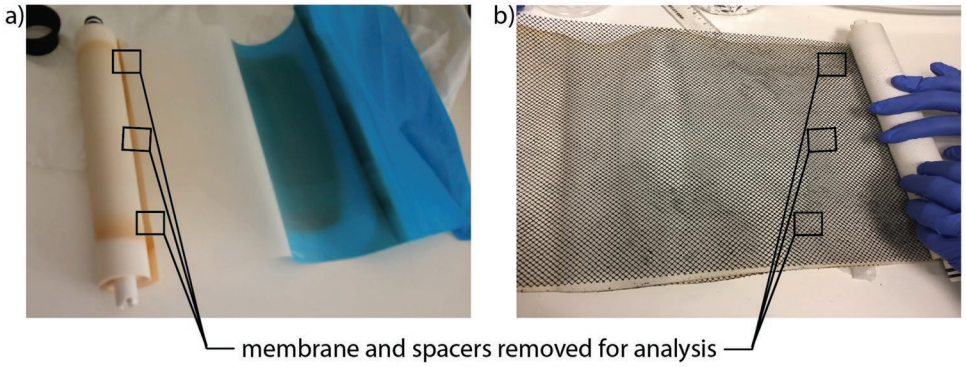

Figure 3. Spiral wound modules were autopsied after biofouling assay. a) Control biofouled membrane with uncoated spacer. b) Test biofouled membrane with LIG spacer. Indicated areas are approximate places (front, middle, and back) where pieces of the membrane and the spacer were removed for biofilm analysis.

were obtained at the front, center, and end of the module. Samples were analyzed using CLSM, (Zeiss LSM 510, META) for EPS, biofilm biovolume, and for bacterial biofilm morphology. Live/Dead BacLight bacterial viability kit (Thermo Fisher Scientific Molecular Probes, USA) were employed to visualize live and dead bacteria under CLSM as in previous studies.[28,34] Briefly, the spacer samples or membrane coupons were first stained with ConA-Alexa Fluor 633, 3.34 µM SYTO 9, and 20 µM propidium iodide in 0.9% saline solutions and incubated for 30 min protected from light. Samples were then washed with 0.9% NaCl and analyzed using CLSM (20×) with a 0.5 numerical aperture. An excitation wavelength of 488 nm was used for both the SYTO 9 and the PI, and 633 nm was used for the Alexa Fluor 633. The biovolume was then determined with Imaris–Bitplane software (Zurich, Switzerland). The threshold was fixed for all image stacks. The extracellular polymeric substances (EPS) on the fouled membrane and spacers were extracted as previously described,[35] the resulting extract was filtered (0.45 µm), and TOC was measured using a total organic carbon analyzer (TOC VCPH, Shimadzu, Kyoto, Japan). Samples were also imaged using SEM as follows. Samples were fixed with 2% paraformaldehyde and 2.5% glutaraldehyde and

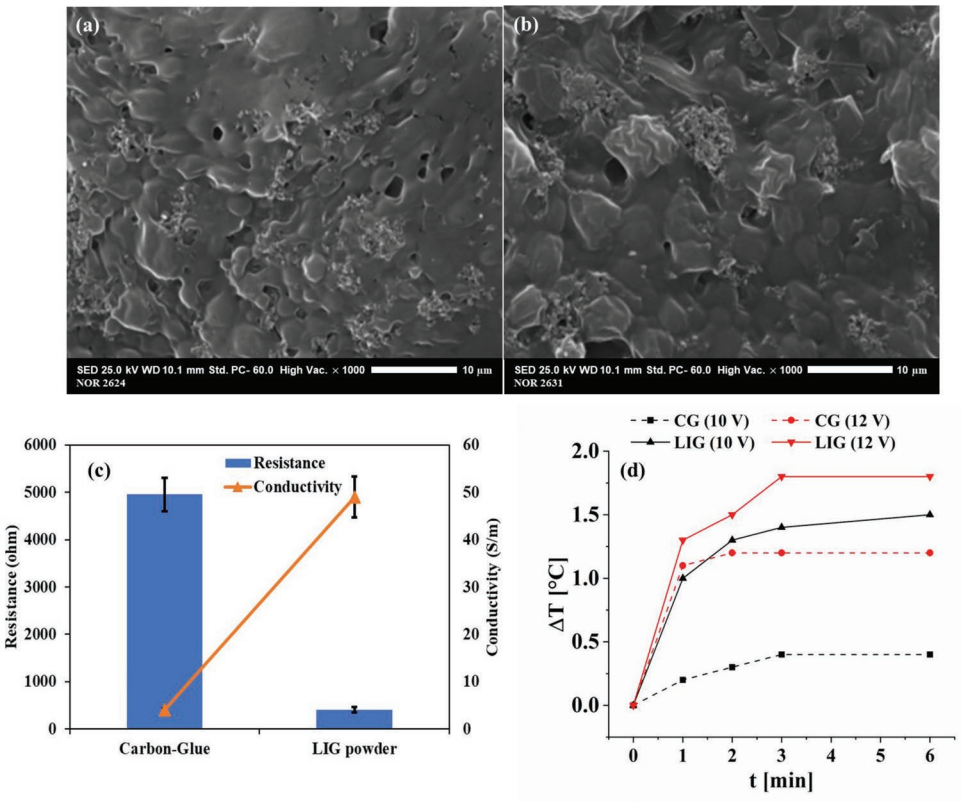

Figure 4. SEM images of the coated feed spacers. a) Carbon-glue coated spacer. b) LIG coated spacer. c) Resistance and electrical conductivity of the modified spacers. d) Heating effects of the coated spacers at 10 V (black) and 12 V (red).

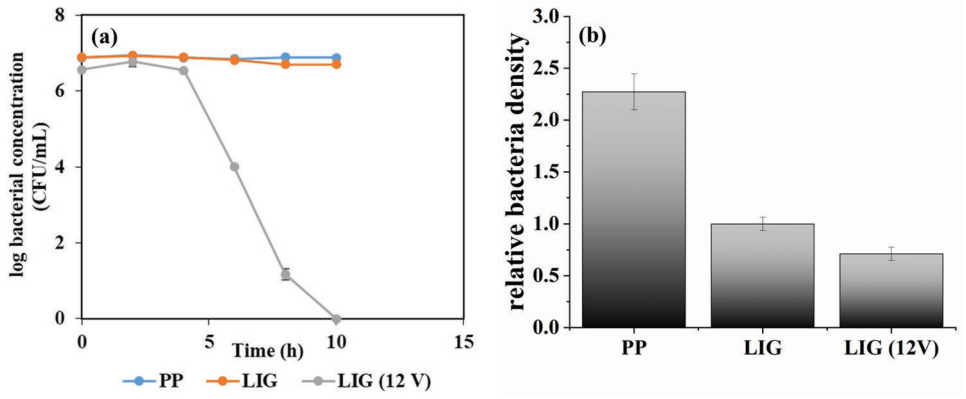

Figure 5. Bacterial inactivation on LIG modified feed spacers with and without electrical potential (12 V) compared with unmodified PP feed spacer. LIG modified feed spacer a) batch study with *Pseudomonas aeruginosa*. b) Adhesion of *Rheinheimera sp.* to LIG modified feed spacers with and without electrical potential (12 V) compared with unmodified PP feed spacer. *Rheinheimera sp* attachment relative bacteria densitiy to LIG (0 V).

thereafter dehydrated using ethanol and finally dried prior to SEM analysis (JSM-IT200, JEOL, Tokyo, Japan) as previously described.[28] To avoid charging effects during imaging, the samples were coated with a ≈10 nm thick layer of platinum/gold using sputter-coating deposition.

3. Results and Discussion

3.1. Surface Characterization of Modified Spacer

SEM analysis of the coated spacer revealed that there were no significant morphological differences in the LIG spacer compared to spacers coated with carbon glue (CG) only (**Figure 4**a,b). The unique porous and fibrous structure of LIG normally seen when fabricated on surfaces[21,32,36] is lost when the material is scraped from the surface and mixed with the carbon glue. The LIG spacer surface was rougher compared to CG only and indicated that the LIG powder contained larger particles. Typically, it has been observed that higher surface roughness aids fouling on the membrane surfaces. However, in the current study even though LIG coated spacer had higher roughness, the fouling was lower compared to the PP spacer. The LIG spacer was ≈5 x more conductive than the spacer coated with carbon glue only (Figure 4c). At the same voltage, a spacer with higher electrical conductivity will have a higher electric current, and increased electrical effects are possible.[30] When 10 and 12 V were applied to the spacers with different resistances in air, ≈2500, and ≈500 Ω for carbon glue and LIG spacers, respectively, only small temperature increases were observed (0.4–1.8 °C) (Figure 4d) and indicated that temperature and heating effects would not play a role in antimicrobial or antibiofouling activity of the LIG spacers.

3.2. Antibacterial Activity of CG LIG

Bacterial inhibition experiments performed using *Pseudomonas aeruginosa* as a model organism suggested that the LIG spacer was capable of reducing bacterial viability in the batch mode (**Figure 5**a). Complete inactivation of the bacteria was observed when 12 V was applied for 10 h. It has been reported that the electric effect in combination with LIG surface effects results in irreversible damage to the bacterial cells, and electric current was observed to kill bacteria.[28,30] In the capacitive mode electrical application, the mechanism of inactivation occurs by direct oxidation, which damages the cell wall, and secondly indirect oxidation by the generation of biocides.[33] In a resistive mode electrical application, bacterial inactivation is mainly due to direct oxidation. Also, it was observed that the application of a low voltage to LIG surfaces for 4 h in different configurations resulted in a ≈4 log reduction of bacterial viability (*Pseudomonas aeruginosa*).[28]

3.3. Bacterial Adhesion Assay

We then performed a dynamic accumulation assay using the brackish water bacteria *Rheinheimera sp.* using the LIG feed spacer with an applied potential of 12 V, which showed the lowest bacterial adhesion compared to both the unmodified PP feed spacer and the LIG spacer with no electric current (Figure 5b). The electrified LIG feed spacer reduced bacterial adhesion by 69% compared to the unmodified PP feed spacer, which showed the highest amount of bacterial adhesion. In comparison, the LIG-coated feed spacer with no electric current showed a 56% reduction of bacterial adhesion when compared to PP. Thus, the electrical effects significantly reduced the number of bacteria on the surface by 29% ($p < 0.05$). These results agree with a previous study, which showed the anti-biofouling properties of LIG, where biofilm growth on the LIG electrodes was found to be reduced compared to PI or graphite. Wherein the antibiofouling property of LIG was attributed to enhanced hydrophilicity and increased negative charge on LIG that ultimately resulted in electrostatic repulsion of bacteria.[28] Although the extreme antifouling properties of LIG are reduced if incorporated into a composite material, they can be optimized by tailoring the ratio of the LIG in the composite material.[37] Thus in the present case, the antifouling effects of the LIG seem to be masked when composited with the carbon glue because the structure and chemistry of the LIG are not present at the surface-water interface. Yet, the increased

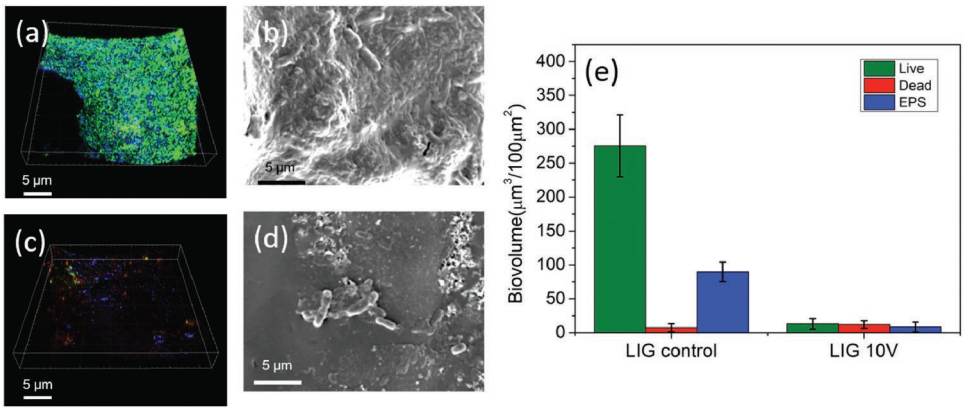

Figure 6. Biofouling analysis on the LIG spacer surfaces. Biofilm growth conditions include *P. aeruginosa* inoculation and incubation at 30 °C for 72 h in a flow-through mode. CSLM and SEM images a,b) control LIG and c,d) LIG with 10 V electric field through resistor mode. e) IMARIS quantification of the biofilm volume showing the live bacteria (green), dead bacteria (red), and extracellular polymeric substance (EPS) (blue).

electrical conductivity of the LIG spacer allowed the application of low currents at lower voltages, which enhanced antibacterial and antifouling effects.

3.4. LIG Spacer Biofouling Prevention in the Flat Sheet Module

In order to test the spacer in dynamic flow conditions, the anti-biofouling activity of the LIG feed spacer was investigated in cross flow-through mode using feed water containing a model bacterial *P. aeruginosa* in which 10 V was applied to the LIG spacer in a resistive mode.[33] After 72 h, samples were analyzed using CSLM and SEM and the amount of biofilm was quantified (**Figure 6**). There was significantly less biofilm and bacterial adherence observed on the LIG spacer with 10 V electric field application (Figure 6c–d) compared to the control LIG spacer (no electricity), which showed bacterial attachment and biofilm growth, in which 280 ± 50 μm^3 biovolume was observed for the 10 μm^2 area (Figure 6a,b). In contrast, almost no biofilm was formed on the LIG spacer when an electrical current was present.

The mechanism of antibacterial and biofouling properties of conductive surfaces in presence of resistive mode electric current is not fully understood.[33] We test here only in a resistive mode electrical circuit, where electrons can flow through both the LIG spacer and the electrolyte solution. Compared with a capacitor mode configuration, the electrons flow only through the electrolyte.[33,38] Although charged surfaces and ROS bursts are associated with a capacitive mode,[30] we find here that previous studies have shown that antimicrobial effects other than resistive heating are associated with the resistor mode.[33,39] In this work, Ohmic heating in the air was very low; the measured temperature was increased slightly (0.4–1.8 °C) at 10–12 V, and therefore, the heating of the surface underwater is expected to be even lower. Moreover, rapid heat dissipation would be expected in the membrane system studied due to the high volumes of recirculated water. Bacterial cell inactivation due to Ohmic heating is described at electric field strengths above 30 V cm^{-1} and temperature above 50 °C, at a rate proportional to the electrical conductivity of the medium.[33,40] In this present case, we hypothesize that the direct oxidation and other electric effects at higher voltage (10 V) are the factors for the significant anti-biofouling properties. However, subsequent in-depth studies are needed to better understand the mechanism of the anti-biofouling behavior of resistive mode LIG spacers.

3.5. LIG Modified Feed Spacer Biofouling Assay in a Spiral Wound RO Module

Various studies have been focused on developing electrically conductive spacers and membranes for reduced biofouling on the membrane surface.[41,28] Baek et al.[42] fabricated a spiral wound membrane with Titanium mesh as an alternative for conventional feed spacers and observed reduced biofouling on the membrane surface when paired with a counter electrode. However, the fabrication of spiral wound membrane modules containing conductive feed spacers, tested using contaminated water under pressure with simultaneous electrical current through the spacer used in a resistor configuration has not been reported to the best of our knowledge. Thus we fabricated spiral wound membrane modules containing the electrically conductive LIG-modified feed spacer. The major challenge with the concept of electrically conductive components in water treatment technology is the electrical connections to an external electrical source, and here we needed to connect an electric source to the feed spacer within the pressurized module housing. Nonetheless, steel wires in silicon tubing were attached to each side of the spacer on either side of the module. A hole was drilled in the housing for one of the wires, while the other wire was threaded through the retentate exit using a 3-way valve (Figure 2). The crossflow biofouling tests were conducted at a constant flux on the spiral wound RO membranes. Brackish water with a natural consortium of brackish water bacteria was used and for a membrane module with an uncoated PP spacer, significant amounts of biofilm growth were observed on the membrane and the spacer in only 48 hours (Figure S2, Supporting Information). Thus, these conditions were chosen to test the LIG spacers. However, under the conditions tested, no significant increase was seen in the operating pressure, which was measured at ≈4 bar after 48 h (Figure S3, Supporting Information), and indicated that membrane fouling was in its initial stage.

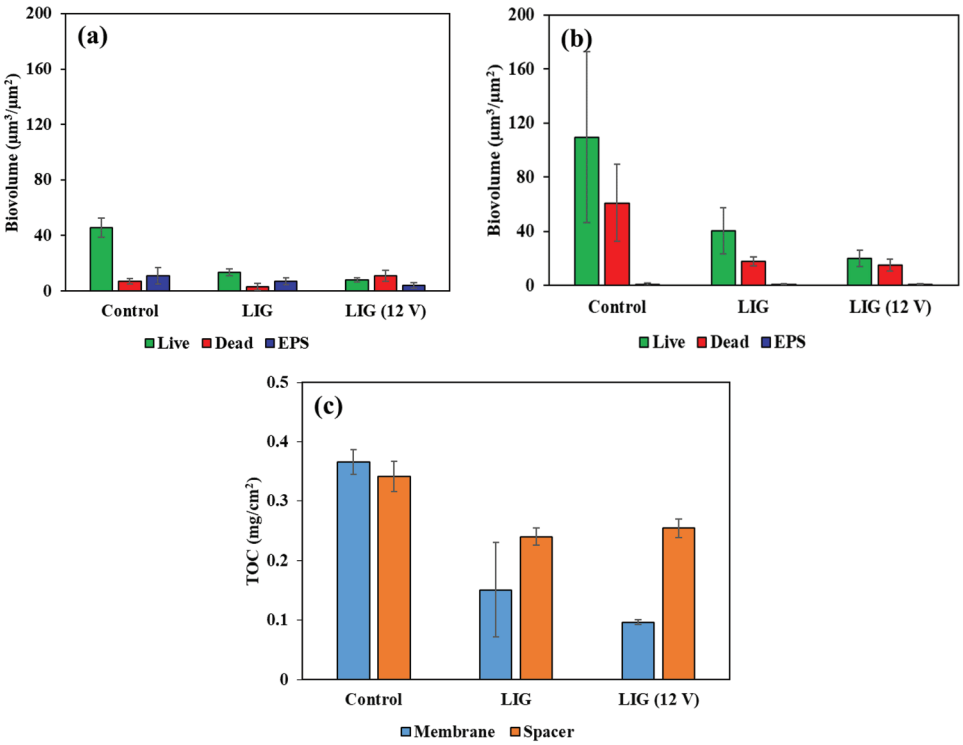

Figure 7. Comparison of biofilm growth on a) membrane and b) spacer. c) TOC extracted from membrane and spacer.

Next, using the same fouling protocol, the performance of the module containing the electrified (12 V) LIG spacer was compared with a module containing the unmodified spacer and the LIG spacer in the absence of an electric field. The membrane modules were removed from the housing and a membrane autopsy was performed, where samples of the membrane and the spacer were taken near the front, in the middle, and near the back end of the membrane module. In general, CLSM analysis revealed biofouling on both the membrane and the spacer components, however, in all cases compared to the

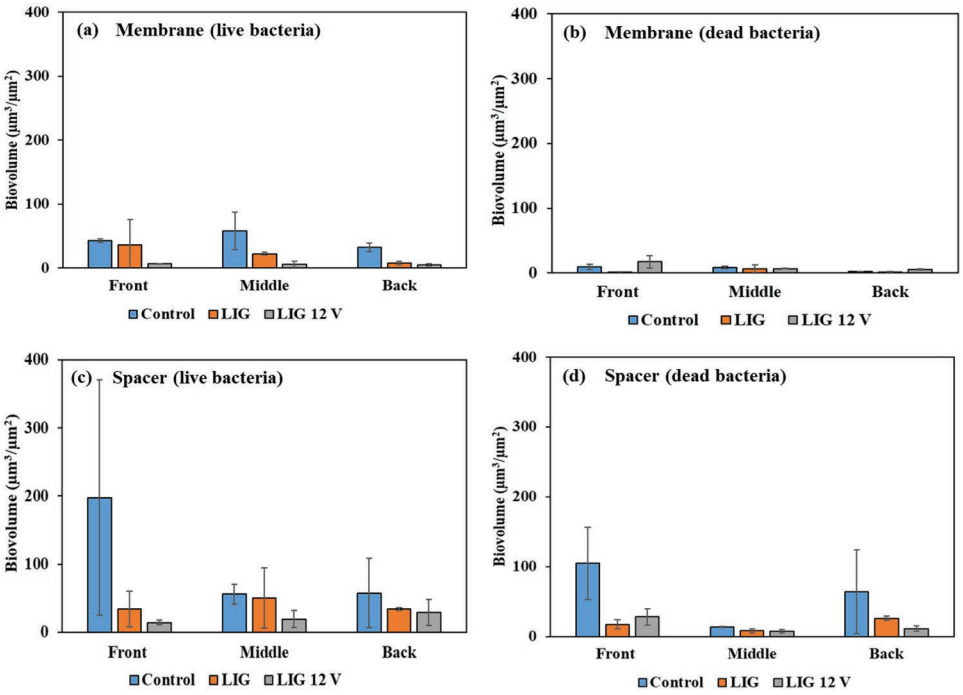

Figure 8. Biofilm analysis (CLSM) for the live (a,c) and the dead (b,d) bacterial volume across the membrane (a,b) and spacer (c,d).

control module, significantly reduced biofilm growth on all components was observed in the module containing the electrified spacer (**Figures 7** and **8**). Similar to the bacterial deposition studies, the LIG-coated spacer without electricity was more effective than the uncoated PP control spacer at reducing biofilm formation, and the additional role of the electricity further reduced biofilm growth. It was also observed that the biovolume, including dead and live bacteria, and EPS components was consistently higher on the spacer compared to that of the membrane and suggests that the spacer component is more susceptible to biofilm growth than the membrane component in the module (Figures 7 and 8). However, for both the spacer and the membrane, the electrical effects reduced live bacteria proportionally from the control module: for the membrane and the spacer, an 82.7% reduction and an 81.8% reduction were seen, respectively.

In general, it is known that biofilm and bacterial attachment occurs on the front part of the module, and scaling occurs toward the back of the module where salinity increases.[43] Similarly, in the current study, for the control spacer, we observed that the biovolume on the front of the spacer was 3x higher than near the middle or back part of the module (Figure 8). However, for the membrane, only minor differences were seen comparing the front, middle, and back of the membrane, which might be due to the short duration (48 h) of the fouling study. Thus, for the LIG spacer with electricity, the biovolume of live bacteria was much more drastically reduced (93%) in the front of the spacer due to this enhanced biofouling near the front of the control module, whereas less drastic yet significant reductions were seen comparing the middle (66%) and the back part (49%) of the module. Overall, the LIG spacers with electric current were found to consistently lower biofilm growth when compared to the PP spacer.

Although EPS on the fouled membrane and spacers could be estimated with CLSM, the EPS was also extracted and quantified using TOC measurements (Figure 7c). CLSM staining, in all cases, gave similar, albeit decreasing amounts of EPS on the membrane and spacer components compared to the control module, and TOC revealed a similar trend. Both the LIG spacer with and without electricity gave less EPS than the control and indicated less bacterial attachment to the components and delayed biofilm growth.

4. Conclusion

Biofouling remains an ongoing challenge in membrane separation processes. In this work, a LIG feed spacer was fabricated and demonstrated antibiofouling when connected as a resistor while applying 10–12 V. Until now, electrically conductive water technologies were not tested in spiral wound configurations because of the challenge to connect the module components to an external electric potential. The LIG-coated feed spacer was scaled up and tested in a RO spiral wound module and connected to an external electrical source through modification of the module housing. Electrically dependent biofouling control was observed using a bacterial consortium isolated from real brackish water, and the fouling was performed with brackish water obtained from the same source. Compared to other biofouling control strategies or processes that require frequent chemical cleaning and backwashing, an electrified LIG spacer, fabricated using a low-cost LIG carbon glue composite can inspire potentially new electrically dependent anti-biofouling technologies.

Supporting Information

Supporting Information is available from the Wiley Online Library or from the author.

Acknowledgements

L.P. and C.T. contributed equally to this work. This research was supported by a grant from the Ministry of Science and Technology of the State of Israel and the German Federal Ministry of Education and Research (BMBF, PTKA), BMBF 02WIL1487. The authors thank Aqua Membranes, Inc. (Albuquerque, USA) for fabrication and provision of the spiral wound modules.

Conflict of Interest

The authors declare no conflict of interest.

Data Availability Statement

The data that support the findings of this study are available from the corresponding author upon reasonable request.

Keywords

biofilm inhibition, feed spacers, laser-induced graphene, spiral wound modules, water treatments

Received: June 30, 2022
Revised: September 21, 2022
Published online:

[1] M. Henmi, Y. Fusaoka, H. Tomioka, M. Kurihara, *Water Pract Technol* **2009**, *4*, wpt2009068.
[2] M. Al-Abri, B. Al-Ghafri, T. Bora, S. Dobretsov, J. Dutta, S. Castelletto, L. Rosa, A. Boretti, *npj Clean Water* **2019**, *2*, 2.
[3] N. P. Isaias, *Desalination* **2001**, *139*, 57.
[4] J. Gutman, M. Herzberg, S. L. Walker, *Environ. Sci. Technol.* **2014**, *48*, 13941.
[5] A. Al Ashhab, A. Sweity, B. Bayramoglu, M. Herzberg, O. Gillor, *Biofouling* **2017**, *33*, 397.
[6] H. C. Flemming, J. Wingender, *Nat. Rev. Microbiol.* **2010**, *8*, 623.
[7] S. Bucs, N. Farhat, J. C. Kruithof, C. Picioreanu, M. C. M. van Loosdrecht, J. S. Vrouwenvelder, *Desalination* **2018**, *434*, 189.
[8] J. R. Werber, C. O. Osuji, M. Elimelech, *Nat. Rev. Mater.* **2016**, *1*, 16018.
[9] Y. N. Kwon, S. Hong, H. Choi, T. Tak, *J Memb Sci* **2012**, *415-416*, 192.
[10] S. R. Suwarno, X. Chen, T. H. Chong, D. McDougald, Y. Cohen, S. A. Rice, A. G. Fane, *J Memb Sci* **2014**, *467*, 116.
[11] M. Chakraborty, M. S. J. Hashmi, *Adv. Mater. Process. Technol.* **2018**, *4*, 573.
[12] C. Liao, Y. Li, S. C. Tjong, *Int. J. Mol. Sci.* **2018**, *19*, 3564.

[13] C. Yang, M. E. Denno, P. Pyakurel, B. J. Venton, *Anal. Chim. Acta* **2015**, *887*, 17.
[14] G. Divyapriya, P. V. Nidheesh, *ACS Omega* **2020**, *5*, 4725.
[15] S. Singh, A. G. Anil, S. Khasnabis, V. Kumar, B. Nath, V. Adiga, T. S. S. Kumar Naik, S. Subramanian, V. Kumar, J. Singh, P. C. Ramamurthy, *Environ. Res.* **2022**, *203*, 111891.
[16] I. E. Mejías Carpio, C. M. Santos, X. Wei, D. F. Rodrigues, *Nanoscale* **2012**, *4*, 4746.
[17] J. Chen, H. Peng, X. Wang, F. Shao, Z. Yuan, H. Han, *Nanoscale* **2014**, *6*, 1879.
[18] F. Perreault, A. F. De Faria, S. Nejati, M. Elimelech, *ACS Nano* **2015**, *9*, 7226.
[19] F. Cui, T. Li, D. Wang, S. Yi, J. Li, X. Li, *J. Hazard. Mater.* **2022**, *431*, 128597.
[20] F. Antonio Gomes da Silva, K. E. Eckhart, M. Matiuzzi da Costa, S. A. Sydlik, H. Pequeno de Oliveira, *Appl. Surf. Sci.* **2022**, *576*, 151768.
[21] S. P. Singh, S. Ramanan, Y. Kaufman, C. J. Arnusch, *ACS Appl. Nano Mater.* **2018**, *1*, 1713.
[22] C. Martini, F. Longo, R. Castagnola, L. Marigo, N. M. Grande, M. Cordaro, M. Cacaci, M. Papi, V. Palmieri, F. Bugli, M. Sanguinetti, *Antibiotics* **2020**, *9*, 692.
[23] D. C. Marcano, D. V. Kosynkin, J. M. Berlin, A. Sinitskii, Z. Sun, A. Slesarev, L. B. Alemany, W. Lu, J. M. Tour, *ACS Nano* **2010**, *4*, 4806.
[24] A. T. Habte, D. W. Ayele, M. Hu, *Adv. Mater. Sci. Eng.* **2019**, 5058163.
[25] R. Arvidsson, D. Kushnir, B. A. Sandén, S. Molander, *Environ. Sci. Technol.* **2014**, *48*, 4529.
[26] R. Ye, D. K. James, J. M. Tour, *Adv. Mater.* **2019**, *31*, 1803621.
[27] J. Lin, Z. Peng, Y. Liu, F. Ruiz-Zepeda, R. Ye, E. L. G. Samuel, M. J. Yacaman, B. I. Yakobson, J. M. Tour, *Nat. Commun.* **2014**, *5*, 5714.
[28] S. P. Singh, Y. Li, A. Be'Er, Y. Oren, J. M. Tour, C. J. Arnusch, *ACS Appl. Mater. Interfaces* **2017**, *9*, 18238.
[29] N. Dixit, S. P. Singh, *ACS Omega* **2022**, *7*, 5112.
[30] A. Gupta, C. P. Sharma, C. Thamaraiselvan, L. Pisharody, C. D. Powell, C. J. Arnusch, *ACS Appl. Mater. Interfaces* **2021**, *13*, 59373.
[31] C. Thamaraiselvan, E. Manderfeld, M. N. Kleinberg, A. Rosenhahn, C. J. Arnusch, *ACS Appl. Bio. Mater.* **2021**, *4*, 4191.
[32] C. Thamaraiselvan, A. K. Thakur, A. Gupta, C. J. Arnusch, *ACS Appl. Mater. Interfaces* **2021**, *13*, 1452.
[33] C. Thamaraiselvan, A. Ronen, S. Lerman, M. Balaish, Y. Ein-Eli, C. G. Dosoretz, *Water Res.* **2018**, *129*, 143.
[34] A. Lakretz, H. Mamane, E. Asa, T. Harif, M. Herzberg, *Environ. Sci.* **2018**, *4*, 1331.
[35] H. Liu, H. H. P. Fang, *J. Biotechnol.* **2002**, *95*, 249.
[36] S. P. Singh, Y. Li, J. Zhang, J. M. Tour, C. J. Arnusch, *ACS Nano* **2018**, *12*, 289.
[37] A. K. Thakur, S. P. Singh, M. N. Kleinberg, A. Gupta, C. J. Arnusch, *ACS Appl. Mater. Interfaces* **2019**, *11*, 10914.
[38] L. Jiang, L. Chen, L. Zhu, *Water Res.* **2019**, *161*, 297.
[39] A. Ronen, W. Duan, I. Wheeldon, S. L. Walker, D. Jassby, *Environ. Sci. Technol.* **2015**, *49*, 12741.
[40] C. Jiménez-Sánchez, J. Lozano-Sánchez, A. Segura-Carretero, A. Fernández-Gutiérrez, *Crit. Rev. Food Sci. Nutr.* **2017**, *57*, 501.
[41] B. S. Lalia, F. E. Ahmed, T. Shah, N. Hilal, R. Hashaikeh, *Desalination* **2015**, *360*, 8.
[42] Y. Baek, H. Yoon, S. Shim, J. Choi, J. Yoon, *Environ. Sci. Technol. Lett.* **2014**, *1*, 179.
[43] T. Nguyen, F. A. Roddick, L. Fan, *Membranes (Basel)* **2012**, *2*, 804.